

NUMERICAL INVESTIGATION OF ENHANCED OIL RECOVERY WITH STEAM INJECTION

AdeyinkaAyoadeAdegbola¹

GaniyuOlajide²

Lateef OwolabiMudashiru³

OyetundeAdeoyeAdeaga⁴

Abstract

Crude oil has remained one of the major mineral resources with maximum effect on the economy of its producing countries and the world at large. For continuous oil production, there is need for application of various techniques at different oil production stages. Steam injection appears to be one of the prominent methods applied in reservoir oil recovery whose strength is also harnessed in this article. A three dimensional graphics model was developed using computational fluid dynamics software capable of handling both Newtonian and Non Newtonian fluids. Initial conditions were spelled out and the properties of heavy oil specified. Steam chamber was specified into which steam particles were injected. The governing equations for the models were developed. Also cumulative frequency temperature decreases with time across the cells. During steam injection in a reservoir, oil saturation decreases with time. It was noticed that the recovery factor increases initially to a certain level before decreasing because of the reduction in the steam temperature. The simulation result further shows that accumulation oil production increases along the length of the cell. The simulation results have demonstrated that the steam injection is an effective technique in improving oil recovery.

Keywords: Recovery Factor, Reservoir, Oil Recovery, Steam Injection, Oil Production

¹ **Department of Mechanical Engineering, Ladoke Akintola University of Technology Ogbomoso**

² **Department of Mechanical Engineering, Kwara State Polytechnic, Ilorin**

³ **Department of Mechanical Engineering, LadokeAkintola University of Technology Ogbomoso**

⁴ **Department of Mechanical Engineering, The Ibarapa Polytechnic, Eruwa**

Introduction

Crude oil and natural gas are found in large underground deposits (usually termed reservoirs or pools) in sedimentary basins around the world. The largest oil reservoir in the world (the Arab D limestone in Ghawar in Saudi Arabia) is approximately 230 km long and 30 km wide and 90 m thick. While most commercially exploited minerals and ores exist as solid rocks and have to be physically dug out of the ground, oil and gas exist as fluids underground. They occupy the connected pore space within strata of sedimentary rocks typically sandstones or carbonates. In most oilfields, the pressure gradients are maintained by injecting another fluid (usually water but sometimes gas and termed 'water flooding' or 'gas flooding', respectively) into the reservoir through injection wells. The injected water displaces the oil and occupies the pore space that is originally occupied. By contrast, gas fields are normally exploited simply by reducing the pressure at the production well using compressors. The gas in the reservoir expands as the pressure drops and thus flows to the production well. In order to continue to produce oil there is a need for different techniques that can be applied in successive stages. A first stage is primary recovery followed by secondary recovery and tertiary recovery. During the primary recovery stage, a reservoir drive comes from a number of natural mechanisms. These include natural water displacing oil downward into the well, expansion of the natural gas at the top of the reservoir, expansion of gas initially dissolved in the crude oil, and gravity drainage resulting from the movement of oil within the reservoir from the upper to the lower part where the wells are located. Recovery factor (RF) during the primary recovery stage is typically 5-51%. Over the lifetime of the well the pressure will fall, and at some point there will be insufficient underground pressure to force the oil to the surface. After natural reservoir drive dimensions, secondary recovery methods are applied. They rely on the supply of external energy into the reservoir in the form of injecting fluid to increase reservoir pressure, hence replacing or increasing the natural reservoir drive with an artificial drive. Secondary recovery techniques increase the reservoir's pressure by water injection, natural gas reinjection and gas lift which injects air, carbon dioxide or some other gas into the bottom of an active well, reducing the overall density of fluid in the wellbore. Typically recovery factor (RF) from water-flood operation is about 30% depending on the properties of oil and the characteristics of the reservoir rock. On the average, RF after both operations is between 35 and 45%.

Enhanced or Tertiary oil recovery method increases the mobility of the oil in order to increase extraction. Thermal enhanced oil recovery (TEOR) methods are tertiary recovery techniques that heat the oil, thus reducing its viscosity and making it easier to extract. Steam injection is the most common form of TEOR and is often done with a cogeneration plant. In this type of cogeneration plant, a gas turbine is used to generate electricity and the waste heat. It is used to produce steam, which is then injected into the reservoir. Enhanced oil recovery (EOR) involves injecting a fluid into an oil reservoir that increase oil recovery over that which would be achieved from just pressure maintenance by water or gas injection. For lighter oils, these processes include miscible gas injection, water alternating gas (WAG) injection, polymer flooding, flow diversion via polymer gels and the use of surfactants. For more viscous (so-called heavy) oils these processes include steam injections and air injection (leading to in situ combustion). The majority of EOR processes used today were first proposed in the early 1970s at a time of relatively high oil prices.

Most of the primary source of oil production of well has already being explored and there is hardly any new oil field that has not being explored except those of the environmental unfriendly regions of the world like the Arctic and the Antantic region. In most cases after a first technique to extract oil from these oil wells is used; the volume of oil that still remains inside these reservoirs can be very significant, achieving values of 40% of the total original volume. In order to continue to produce oil there is a need for different techniques that can be applied in successive stages. A first stage occurs when a free path is built from the reservoir to the surface and then there is a natural pressure gradient that pushes the oil to the producer wedge. In secondary stage, a cheap fluid is injected most of the times this is done with water source this fluid has a low degradation process. Enhance Oil Recovery (EOR) technique can significantly extend global oil reserve once oil prices are high enough to make these technique economical. Steam is injected into the well for certain period of time to heat the oil in the surrounding reservoir to a temperature at which it flows (200-300°C under 1 MPa of injection pressure). When enough amount of steam has been injected, the well is shut down and the steam is left to soak for some time no more than few days. This stage is called soaking stage. The reservoir is heated by steam, consequently oil viscosity decreases. The well is opened and production stage is triggered by natural flow at first and then by artificial lift. The reservoir

temperature reverts to the level at which oil flow rate reduces. Then, another cycle is repeated until the production reaches an economically determined level. Groundwater remediation is the process that is used to treat polluted groundwater by removing the pollutant or converting them to harmless product. From the explanations of Groundwater remediation and that of the enhance oil recovery, it is deduced that while groundwater remediation is to extract the contaminant and pollutant from water to make it save for domestic, agricultural and industrial uses, enhanced oil recovery is to increase the percentage of oil recovered from the oil reservoir. In the study, a three phase, three-dimensional model will be presented in order to inspect the steam injection in the heavy oil reservoir. The objectives of the research work were to:

- (1) study the effect of some important parameters on steam injection performance in the reservoir.
- (2) study the effect of steam injection on oil recovery.
- (3) develop a model for predicting oil production from the reservoir using steam injection.
- (4) develop a reliable model for studying steam injection in heavy oil systems.

Brief review

Most models apply to continuous steam injection, but the principles are identical. Marx and Langehiem (1959) describe a method for estimating thermal invasion rates, cumulative heated area, and theoretical economic limits for sustained hot-fluid injection at a constant rate into an idealized reservoir. Full allowance is made for non-productive reservoir heat losses. In all cases, the heat conduction losses to the overburden and the under burden impose and economic limit upon the size of the area that can be swept from any around one injection. These depend on the reservoir conditions and heat injection rate. Jones (1977) presented a simple cyclic steam model for heavy oil, pressure-depleted, gravity-drainage reservoirs. The Boberg and Lantz (1966) procedure was used as the basis for the reservoir shape and temperature calculations versus time. Here, the only driving force assumed is gravity, and hence, the model tends to calculate lower initial oil rates than observed in the field. For matching, certain empirical parameters are employed.

Van Lookeren (1977) has presented calculation methods for linear and radial steam flow in reservoirs. He assumed immediate gravity overlay of the steam zone and presented analytical expressions to describe interface locus. The steam zone shape is governed by factors. A_{LD} and A_{RD} which are dimensionless parameters that characterize the degree of steam override for linear and radial flow, respectively. A simplistic formulation is given to calculate the average steam zone thickness. Myhill and Stegemeier (1978) presented a model for steam drive correlation and prediction. Assuming a piston like displacement, they modified Mandi and Volek's (1969) method to calculate the steam zone volume. It identifies a critical time beyond which the zone downstream of the advancing front is heated by the water moving through the condensation front. Also, a thermal efficiency of the steam zone is calculated as a function of the dimensionless time and the ratio of the latent heat to the total energy injected. Butler et al (1979) presented theoretical equations for gravity- drainage of heavy-oils during in-situ steam heating. The method described consists of an expanding steam injection and production of oil via the mechanism of gravity-drainage along the steam/oil interface of the steam chamber. The oil is produced through a horizontal well located at the bottom of the steam chamber. Oil flow rate is derived starting from Darcy's law. Heat transfer takes into account the thermal diffusivity of the reservoir and it is proportional to the square root of the driving force. In the case of an infinite reservoir, an analytical dimensionless expression is derived that describes the position of the interface. When the outer boundary of the reservoir is considered, the position of the interface and the oil rate are calculated numerically. Oil production scales with the square root of the height of the steam. An equation describing the growth of the steam chamber is also presented. The method is limited to gravity-drainage and linear flow of heavy-oil from horizontal wells. Jones (1981) presented a steam drive model that is basically a combination of Van Lookeren's (1977) and Myhill and Stegemeier's (1978) methods. It is limited to continuous steam drive and it uses empirical factors to match calculated rate with measured values. Vogel (1982) considered heat calculations for steam floods. Similar to Van Lookeren (1977), this model works on the basic assumption of instantaneous steam rise to the top of the reservoir. After this happens, the steam chamber grows downward at a very low velocity. Heat losses to the adjacent formations are calculated by solving the heat conduction problem from an infinite plane. The model characterizes two main driving forces affecting oil production: gravity-drainage and steam drag. In his conclusions, Vogel says that, above a certain limit, injection rates have little

influence on oil production. Finally, Aziz and Gontigo (1984) presented a model that considers the flow potential to be a combination of pressure drop and gravity forces. The flow equation is derived for oil and water production based on the method illustrated by Butler et al (1979). They solve a combined Darcy flow and a heat conduction problem. The structure of the model is based on Jones (1981) method. Thermal EOR methods are generally applicable to heavy, viscous crudes, and involve the introduction of thermal energy or heat into the reservoir to raise the temperature of the oil and reduce its viscosity. Steam (or hot water) injection and in situ combustion are the popular thermal recovery methods. Three common methods involving steam injection are cyclic steam stimulation (huff and puff), steam flooding and steam assisted gravity drainage (SAGD). In situ combustion involves the injection of air, where the oil is ignited, generates heat internally and also produces combustion gases, which enhance recovery (Donaldson, 1985). Thermal recovery methods are the most best for increasing production from heavy oil reservoirs, because thermal methods reduce the viscosity of heavy oil and increase its mobility and as a result, make the economical use of heavy oil reservoirs possible. Steam injection is currently used as one of the most successful enhanced oil methods for heavy oil reservoirs Butler, (1997). This process involves simultaneous heat, mass and fluid transport in the heavy oil reservoir, which aims to Increase the oil recovery efficiency. It has been widely claimed that viscosity reduction plays a key role in increasing the oil recovery efficiency during thermal processes. Extensive studies have been performed to model steam injection process mathematically for prediction of oil recovery.

Methodology

Numerical modeling of steam injections in heavy oil reservoir has taken different forms and methods over the years. The steam injection technique has been found to be efficiently useful in reducing viscosity of the reservoir mixture through steam soaking.

Model Governing Equations

The simulation software uses the following equations as governing equations for the study. Incorporated into the model development equations are also the flow equations. One of the flow equations the software uses is the Reynolds Averaged Navier-Stokes (RANS) equation for

incompressible fluid and both the Euler and modified Euler's equation for compressible fluid of which heavy oil is one, in conjunction with the continuity and fluid flow equations. It solves divides each portion of the model into finite volumes and then solves each part using the finite volume method which discretizes the model parametrically.

$$p \left(\frac{\partial \bar{u}_i}{\partial t} + \frac{\partial (\bar{u}_j \bar{u}_i)}{\partial x_j} \right) = \frac{\partial}{\partial x_j} \left[\mu \left(\frac{\partial \bar{u}_i}{\partial x_j} \right) - p \bar{u}_j \bar{u}_i \right] - \frac{\partial \bar{p}}{\partial x_i} \quad (1)$$

$$p \left(\frac{\partial \bar{u}_i}{\partial t} + \frac{\partial (\bar{u}_j \bar{u}_i)}{\partial x_j} \right) = \frac{\partial}{\partial x_j} \left(2 \mu s_{ji} - p \bar{u}_j \bar{u}_i \right) - \frac{\partial \bar{p}}{\partial x_i} \quad (2)$$

The above shows the RANS equation as derived from the general Navier- Stokes equation below;

$$p \left[\frac{\partial u}{\partial t} + \frac{\partial (u^2)}{\partial x} + \frac{\partial (uv)}{\partial y} + \frac{\partial (uw)}{\partial z} \right] = \frac{\partial}{\partial x} \left(\mu \frac{\partial u}{\partial x} \right) + \frac{\partial}{\partial y} \left(\mu \frac{\partial u}{\partial y} \right) + \frac{\partial}{\partial z} \left(\mu \frac{\partial u}{\partial z} \right) - \frac{\partial p}{\partial x} \quad (3)$$

$$p \left[\frac{\partial v}{\partial t} + \frac{\partial (vu)}{\partial x} + \frac{\partial (v^2)}{\partial y} + \frac{\partial (vw)}{\partial z} \right] = \frac{\partial}{\partial x} \left(\mu \frac{\partial v}{\partial x} \right) + \frac{\partial}{\partial y} \left(\mu \frac{\partial v}{\partial y} \right) + \frac{\partial}{\partial z} \left(\mu \frac{\partial v}{\partial z} \right) - \frac{\partial p}{\partial y} \quad (4)$$

$$p \left[\frac{\partial w}{\partial t} + \frac{\partial (wu)}{\partial x} + \frac{\partial (wv)}{\partial y} + \frac{\partial (w^2)}{\partial z} \right] = \frac{\partial}{\partial x} \left(\mu \frac{\partial w}{\partial x} \right) + \frac{\partial}{\partial y} \left(\mu \frac{\partial w}{\partial y} \right) + \frac{\partial}{\partial z} \left(\mu \frac{\partial w}{\partial z} \right) - \frac{\partial p}{\partial z} \quad (5)$$

The equation below shows the continuity equations with velocity U a function of u,v,w, three dimensional and density ρ with f_α being the volume fraction.

$$\frac{\partial (f_\alpha \rho_\alpha)}{\partial t} + \nabla \cdot (f_\alpha \rho_\alpha \mathbf{U}_\alpha) = 0, \quad (6)$$

$$\frac{\partial (f_\beta \rho_\beta)}{\partial t} + \nabla \cdot (f_\beta \rho_\beta \mathbf{U}_\beta) = 0, \quad (7)$$

Steam Zone Volume during injection is calculated using the Myhill and Stegemier (1978) approach with the equation below;

$$v_s = \frac{Q_i E_{hs}}{M_T \Delta T} \quad (8)$$

Where E_{hs} is the thermal efficiency, ΔT is the temperature rise of the steam zone above the initial reservoir temperature and M_T being the total volumetric heat capacity of the reservoir.

$$M_T = (1 - \phi) M_{rr} + \sum_{\beta=w,o,g} \phi S_\beta M_\beta \quad (9)$$

Where ϕ is the porosity and S being the phase saturation and the subscript β being the individual phases involved.

The heat injection rate is calculated using the equation

$$Q_1 = w_i (C_w \Delta T + f_{sdh} \Delta H_{vdh}) \quad (10)$$

Where w_i is the mass flow rate of the steam injection in the reservoir, C_w is the average specific heat of water over the temperature range corresponding to ΔT with f_{sdh} and H_{vdh} being the steam quality and the latent heat of vaporization respectively. Thus, in the computation as used by the simulation software, the thermal efficiency can be calculated as

$$E_{h,t} = \frac{1}{t_D} \left\{ G(t_D) + (1 - f_{hv}) \frac{U(t_D - t_{oD})}{\sqrt{\pi}} \left[2\sqrt{t_D} - 2(1 - f_{hv})\sqrt{t_D - t_{oD}} - \int_0^{t_D} \frac{e^{-x} \operatorname{erfc}(\sqrt{x})}{\sqrt{t_D - x}} dx - \sqrt{\pi} G(t_D) \right] \right\} \quad (11)$$

The oil and water viscosities using the equation given by Jones (1977) can be calculated as a function of temperature of the medium using the equation below;

$$\mu_o(cp) = 0.001889047 \exp\left(\frac{8956.257}{7 + 460}\right) \quad (12)$$

$$\mu_w(cp) = 0.66 \left[\frac{T}{100} \right]^{-1.14} \quad (13)$$

Where μ_w and μ_o are fluid viscosities of water and heavy oil respectively.

$$API \text{ gravity} = \frac{141.5}{SG} - 131.5 \quad (14)$$

$$\mu_s(\text{Steam viscosity}) = (0.2T + 81.97)(10^4) \quad (15)$$

$T = \text{Temperature in Kelvin}$

Simulation Procedures

In carrying out the modeling and simulation process, the following steps were taken;

- 1) A 3-dimensional model of the reservoir geometry was drawn with dimension 45x 45 x 60 feet using Solidworks Simulation and drafting software. Embedded into it is the steam injection profile of rectangular profile as the steam injection geometry through which the steam injection is introduced as shown in fig 1.
- 2) The model was discretized into cells and nodes through the CFD tessellation algorithm for the purpose of the numerical simulation as shown in the fig. 2. the number of cells created was 1417 in all.

- 3) Computational domain for the simulation was created with this occupying a dimension of 45 x 45 x 10 ft from the base of the reservoir.
- 4) Input parameters were calculated as tabulated in table 1 below and supplied into the model.
- 5) Computational fluid dynamics package of the software was used with flow in the X-directional domain.
- 6) Heavy oil properties were configured into the engineering library of the software and initial conditions were spelled out as in table 1.
- 7) The flow was not adiabatic but heat transfer was made inherent in the model with heat transfer rate specified for the reservoir. Also, the flow was made a mixture of laminar and turbulent flows and a fully developed flow across the reservoir in the hot region was enhanced.
- 8) With the above configuration, the simulation was run and the results reported in the next chapter.
- 9) Steam was injected into the reservoir through the steam chamber and the effect of this on study properties across the model was observed.

Table 1: Characteristics of Reservoir and Steam

Characteristics	Values
Reservoir Permeability	1.5
Reservoir Porosity	0.2
Initial Water Saturation	0.25
Injected Steam Quality	0.8
Initial Reservoir Temperature	21 °C
Reservoir Dimension	13.716 x 13.716 x 18.288 m
Steam Chamber Dimension	4.572 x 4.572 x 3.048 m
Initial Oil Gravity	13.157 cp
Inlet Mass flow Rate	120 kg/s
Initial Reservoir Temperature	293.2 K
Steam Injection Rate	0.00525 Kg/s
Initial Particle Velocity	0.00525 m/s
Initial Particle Temperature	495.93 K

The above Figure shows the 3 dimensional model. The bigger box depicts the reservoir. Inherent in the reservoir is a smaller box which represents the steam chamber. The reservoir is segmented with another line close to the base at a distance of 10m from the top surface, this represents the volume of the heavy oil technically called the computational domain.

Table 2: System Information

Product	Flow Simulation 2014 SP1.0. Build: 2573
Computer name	HP
User name	USER1
Processors	Intel(R) Celeron(R) CPU N2820 @ 2.13GHz
Memory	1949 MB / 8388607 MB
Operating system	(Build 9200)
CAD version	SolidWorks 2014 SP1.0
CPU speed	2129 (532) MHz

Table 3: General Information

Model	Heavy Oil Reservoir.SLDPRT
Project name	Heavy Oil Simulation
Project path	C:\Users\USER1\Documents\SOLIDWORKS\ Heavy Oil Simulation\1
Units system	SI (m-kg-s)
Analysis type	Internal
Exclude cavities without flow conditions	Off
Coordinate system	Global coordinate system
Reference axis	X

For the purpose of the numerical simulation the following data were also used as input in the simulation package.

INPUT DATA**Initial Mesh Settings**

Automatic initial mesh: On

Result resolution level: 2

Advanced narrow channel refinement: On

Refinement in solid region: Off

Geometry Resolution

Evaluation of minimum gap size: Automatic

Evaluation of minimum wall thickness: Automatic

Computational Domain

The computation was performed as an internal flow problem with the computational domain representing the location of the reservoir as buried underneath the ground surface. The size of the computational domain is depicted in the table below:

Table 4: Size

X min	-6.862 m
X max	6.862 m
Y min	-18.296 m
Y max	-10.000 m
Z min	-6.862 m
Z max	6.862 m

Table 5: Gravitational Settings

X component	0 m/s ²
Y component	-9.81 m/s ²
Z component	0 m/s ²

Default wall conditions

Heat transfer rate: 12400.000 W

BOUNDARY CONDITIONS

Boundary conditions were set in place in the simulation study with inlet mass flow rate specified and the environmental pressure spelled out too as depicted below;

Table 6: Initial Conditions

Thermodynamic parameters	Static Pressure: 101325.00 Pa Temperature: 293.20 K
Velocity parameters	Velocity vector Velocity in X direction: 0 m/s Velocity in Y direction: 0 m/s Velocity in Z direction: 0 m/s
Turbulence parameters	Turbulence intensity and length Intensity: 2.00 % Length: 0.137 m

Material Settings

Fluids:

Heavy Oil

Table 8: Inlet Mass Flow

Type	Inlet Mass Flow
Faces	Face<2>@Shell1
Coordinate system	Face Coordinate System
Reference axis	X
Flow parameters	Flow vectors direction: Normal to face Mass flow rate: 120.0000 kg/s Fully developed flow: Yes Inlet profile: 0
Thermodynamic parameters	Temperature: 293.20 K
Turbulence parameters	Turbulence intensity and length Intensity: 2.00 % Length: 0.137 m
Boundary layer parameters	Boundary layer type: Turbulent

Table 9: Environment Pressure

Type	Environment Pressure
Faces	Face<3>@Boss-Extrude2
Coordinate system	Face Coordinate System
Reference axis	X
Thermodynamic parameters	Environment pressure: 101325.00 Pa Temperature: 293.20 K
Turbulence parameters	Turbulence intensity and length Intensity: 2.00 % Length: 0.137 m
Boundary layer parameters	Boundary layer type: Turbulent

Goals

For the study, global goals which are metrics to be fulfilled during convergence of the study were spelled out to be a maximum fluid flow and heat transfer rate across the model.

Global Goals**Table 10: GG Mass (Fluid) 1**

Type	Global Goal
Goal type	Mass (Fluid)
Coordinate system	Global coordinate system
Use in convergence	On

Table 11: GG Heat Transfer Rate 1

Type	Global Goal
Goal type	Heat Transfer Rate
Coordinate system	Global coordinate system
Use in convergence	On

Calculation Control Options

Conditions for convergence and termination of the simulation process are as below;

Table 12: Finish Conditions

Finish conditions	If one is satisfied
Maximum travels	4
Goals convergence	Analysis interval: 5e-001

Steam was injected in form of particles. The table below shows the coordinates of the injected steam and the residence time in the flow.

Table 13: The coordinates of the injected steam and the residence time in the flow

Trajectories	Length [m]	Residence time [s]	Fate
Injection 1			
#1 (-2.319 m;-17.139 m;-1.829 m)	0.033	64.343	Opening
#2 (-2.319 m;-16.379 m;-1.829 m)	0.033	43.534	Opening
#3 (-2.319 m;-15.620 m;-1.829 m)	0.034	41.875	Opening
#4 (-2.319 m;-17.898 m;-1.829 m)	0.033	123.357	Opening
#5 (-2.319 m;-17.139 m;-0.914 m)	0.033	49.571	Opening
#6 (-2.319 m;-16.379 m;-0.914 m)	0.033	35.034	Opening
#7 (-2.319 m;-15.620 m;-0.914 m)	0.033	37.049	Opening
#8 (-2.319 m;-17.898 m;-0.914 m)	0.033	96.598	Opening
#9 (-2.319 m;-17.139 m;0 m)	0.033	46.403	Opening
#10 (-2.319 m;-16.379 m;0 m)	0.033	33.038	Opening
#11 (-2.319 m;-15.620 m;0 m)	0.033	35.689	Opening
#12 (-2.319 m;-17.898 m;0 m)	0.033	90.724	Opening
#13 (-2.319 m;-17.139 m;0.914 m)	0.033	49.868	Opening
#14 (-2.319 m;-16.379 m;0.914 m)	0.033	35.138	Opening
#15 (-2.319 m;-15.620 m;0.914 m)	0.033	37.086	Opening
#16 (-2.319 m;-17.898 m;0.914 m)	0.033	97.475	Opening
#17 (-2.319 m;-17.139 m;1.829 m)	0.033	64.441	Opening
#18 (-2.319 m;-16.379 m;1.829 m)	0.033	43.473	Opening
#19 (-2.319 m;-15.620 m;1.829 m)	0.034	41.83	Opening
#20 (-2.319 m;-17.898 m;1.829 m)	0.033	124.083	Opening

Results and Discussion

The simulation was run and 40 iterations were performed until convergence is reached and the following results were obtained;

The number of cells generated across the coordinates as below;

Table 11: Basic Mesh Dimensions

Number of cells in X	9
Number of cells in Y	6
Number of cells in Z	9

Table 12: Number of Cells

Total cells	1417
Fluid cells	815
Solid cells	50
Partial cells	552
Irregular cells	0
Trimmed cells	0

Maximum refinement level: 1

Table 13: Goals

Name	Unit	Value	Progress	Use in convergence	Delta	Criteria
GG Mass (Fluid) 1	kg	1469926.082	100	On	0	14699.2608
GG Heat Transfer Rate 1	W	12400.000	100	On	0	3.1

The table below shows the minimum and maximum values of study parameters obtained in the course of the study.

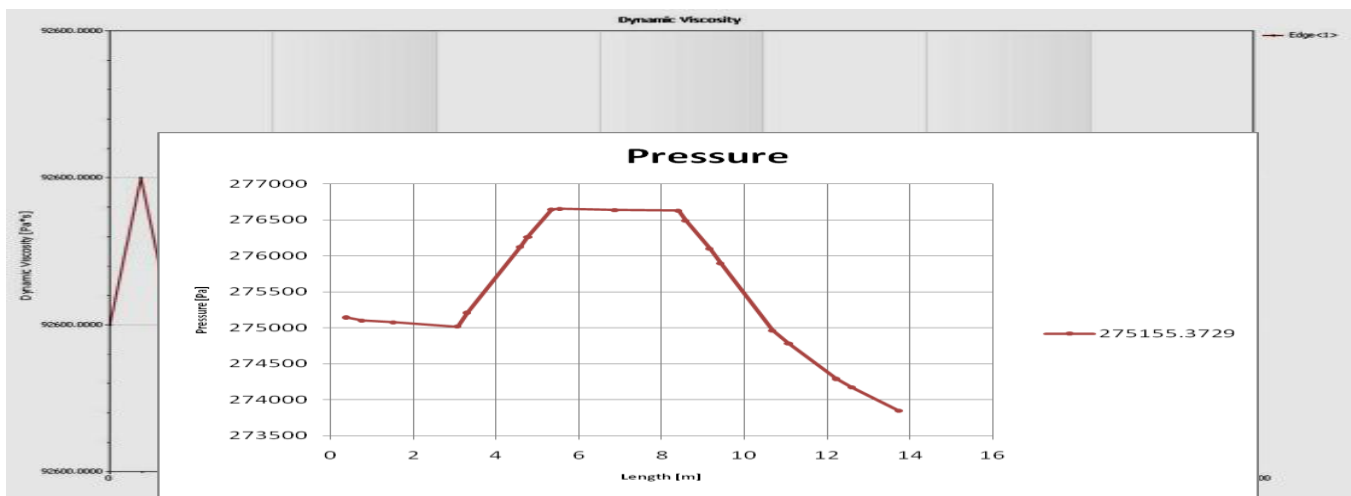
Table 14: Min/Max

Name	Minimum	Maximum
Pressure [Pa]	204853.80	278525.30

Temperature [K]	293.20	293.25
Density (Fluid) [kg/m ³]	987.00	987.00
Velocity [m/s]	0	0.002
Velocity (X) [m/s]	-3.798e-005	0.001
Velocity (Y) [m/s]	-4.130e-005	0.001
Velocity (Z) [m/s]	-5.307e-004	5.283e-004
Temperature (Fluid) [K]	293.20	293.25
Vorticity [1/s]	2.095e-006	0.001
Shear Stress [Pa]	0.11	276.75
Relative Pressure [Pa]	103528.80	177200.30
Dynamic Viscosity [Pa*s]	92600.0000	92600.0000
Heat Transfer Coefficient [W/m ² /K]	410.944	18944.553
Surface Heat Flux [W/m ²]	0	21.778

Fig. 9: Pressure plot across the reservoir length

The temperature gradient across the reservoir was plotted along the XY plane of the model. The



temperature graph is as below and data for the plot put in the appendices.

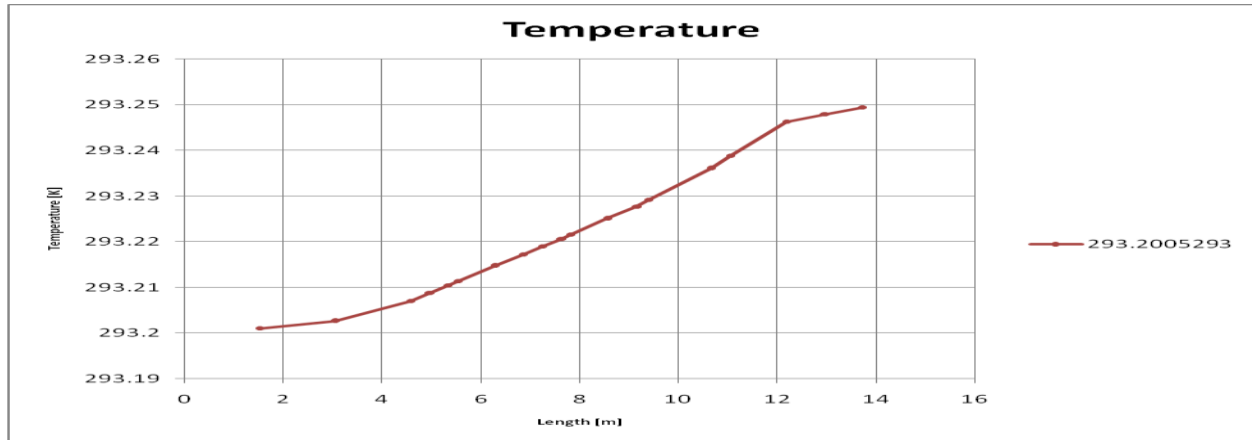


Fig. 10: Temperature plot across the reservoir

The graph of the dynamic viscosity across the model is plotted below;

Fig. 11: Dynamic Viscosity across the reservoir

The above Figure shows that dynamic viscosity of the fluid varies non-linearly across the length of the reservoir as the fluid travels from one end to the other. This parameter is also affected by the temperature gradient across board.

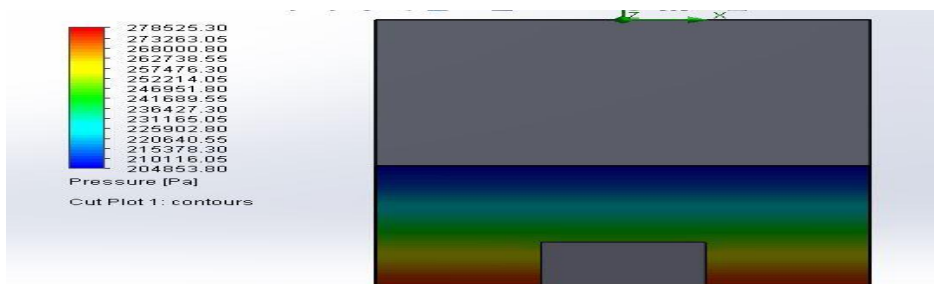


Fig. 12: Pressure Cut Plot

The above Figure shows the pressure plot across the model and the legend also placed beside for easy interpretation of the colour- bar plot.

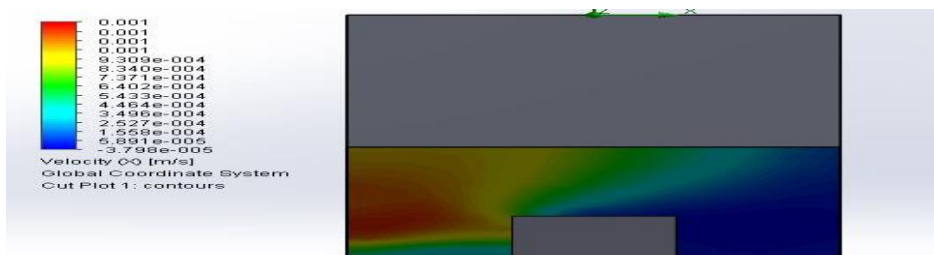


Fig. 13: Velocity Cut Plot

The Figure above (Fig. 4.6) shows the velocity plot of the heavy oil across the reservoir.

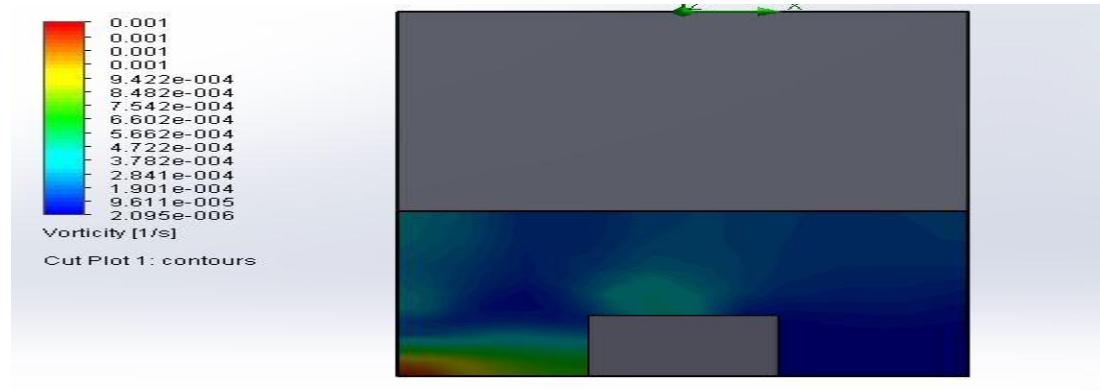


Fig. 15: Vorticity Cut Plot

Figure 15 above shows the vorticity cut plot across the reservoir for the period of study.

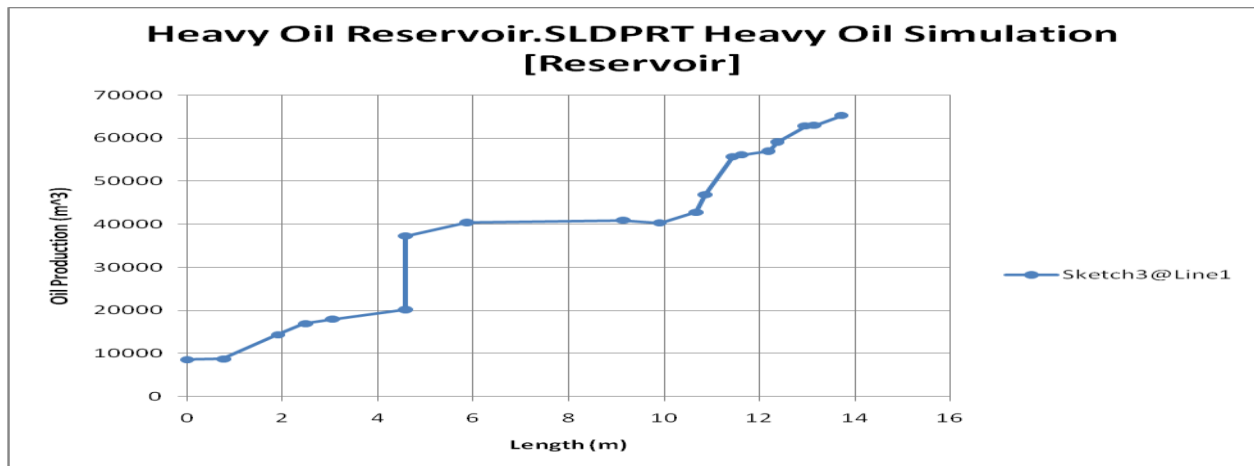


Fig. 15: Heavy oil reservoir

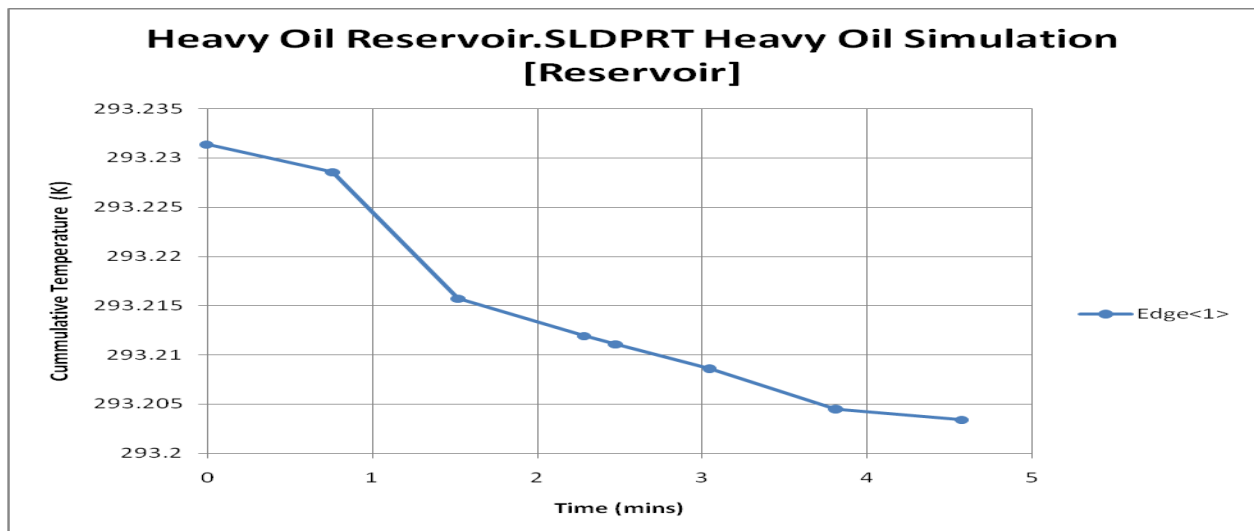


Fig. 16: Heavy oil reservoir. SLDPRT heavy oil simulation.

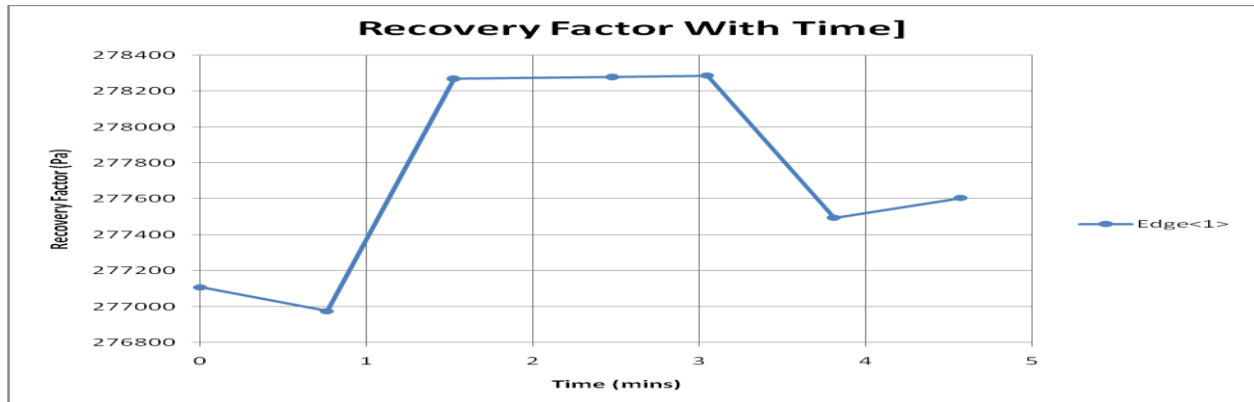


Fig. 17: Recovery factor with time.

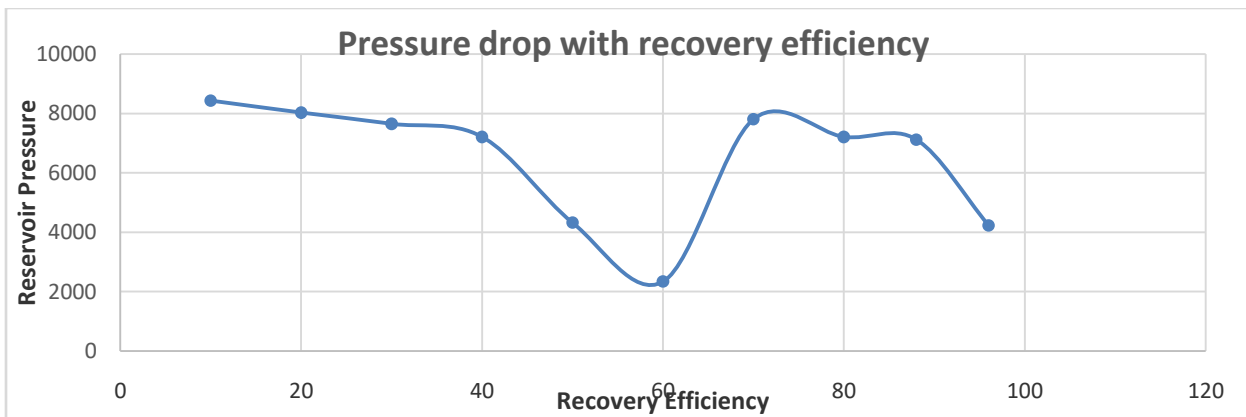


Fig. 20 Pressure drop with recovery efficiency

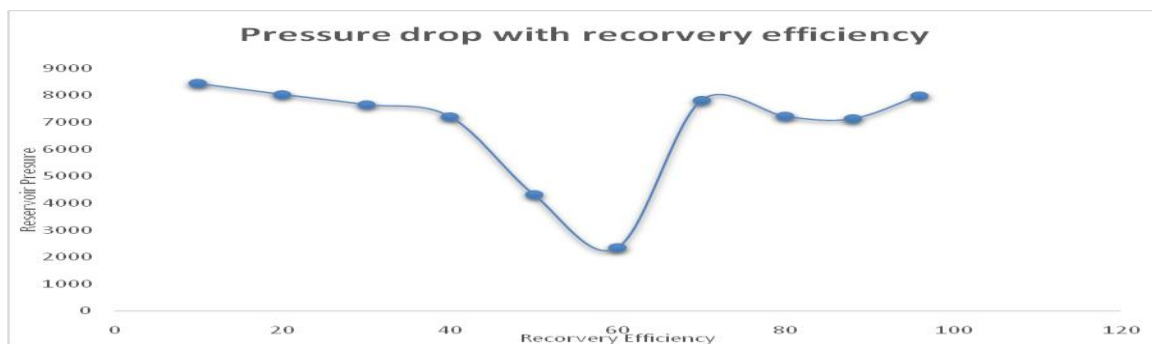


Fig. 21: Pressure drop with recovery efficiency

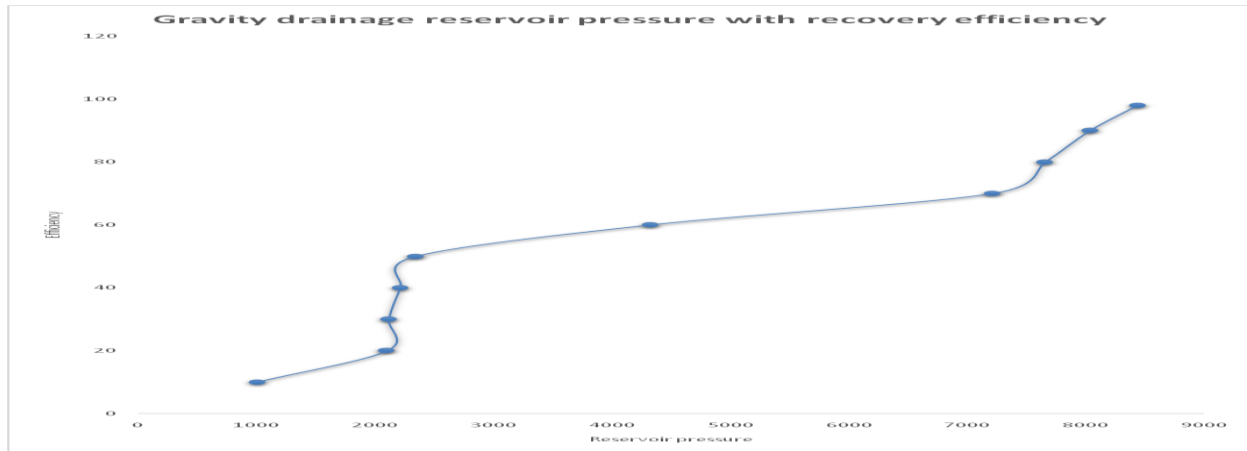


Fig. 22: Gravity drainage reservoir pressure with recovery efficiency.

In Fig. 22 the overall reservoir pressure begins to drop gradually from about 8000 MPa to 7000MPa as soon as oil withdrawal commences and production of natural gas from the reservoir starts and, it occurs at close to 40% recovery efficiency. Later the pressure drops to a remarkable pressure of about 2000MPa when at least more than 40% of the reservoir' s original oil in place has been withdrawn. It is also evident from Fig. 23 that the recovery efficiency had risen apparently. As production continues the reservoir pressure then drops further to about 30% and the recovery rate can only increase at low production rate at the expense of production delay time and production energy dissipation. At this recovery the optimum oil production rate is fully compromised and hence secondary recovery efficiency is necessary. Fig. 23 only corroborate the essence of fig. 22, in order to show that at the initial stage of oil production the recovery efficiency increases because there were large volume of oil in place in the reservoir but recovery efficiency reduces as soon as the reservoir pressure drops below the capillary pressure of oil. Nevertheless the reservoir gas can be present in large volume. To increase the recovery efficiency, the pressure of the reservoir needs to be increased, hence injection method or any other secondary recovery methods. The recovery efficiency is actually a function of reservoir pressure. That is the higher the reservoir pressure, the higher the recovery efficiency as shown in Fig.24. When the production starts, i.e. the withdrawal of oil from the reservoir, the initial pressure pushes out more oil which dictates that we have higher recovery efficiency, but as reservoir pressure drops the production rate drops too which eventually will reduce the recovery efficiency. The three figures obtained above from simulation results definitely describes crude oil recovery efficiency as highly dependent on estimated original oil in place (OOIP), reservoir pressure and the efficacy of the secondary recovery method applied. The estimated original oil in

place (OOIP) actually suggests the likelihood of having higher recovery efficiency, and as such will be used to predict the initial pressure of the reservoir. The larger the quantity of OOIP, the higher the recovery efficiency and of course the more efficient the secondary recovery method employed for optimum oil production in oil reservoir.

Conclusion

This work shows that

- (1) Steam injection can improve oil recovery from nearly zero to around 60% during a fixed period of time.
- (2) The cumulative temperature decreases with time across the cells.
- (3) During steam injection in a reservoir, oil saturation decreases versus time.
- (4) The recovery factor increases initially to a certain level before decreasing because of the reduction in the steam temperature.
- (5) Cumulative oil production increases along the length of the cell.
- (6) Numerical simulation showed that the superheated steam chamber existed within 3m underground in the near wellbore area, therefore, the real superheated steam injection would be realized at the reservoir.

Recommendations for future Research

Enhance oil recovery techniques are very sensitive to geological heterogeneity and so additional work must be performed to evaluate reservoir description before development proceeds.

- (1) New EOR technologies are needed that are easier to design, require less specialist equipment and produce a quicker response in terms of oil rate. This is particularly the case for mature off-shore fields where there is little space for additional equipment on platforms.
- (2) This also suggests that companies should be planning the deployment of both new and existing EOR technologies at the beginning of field development to ensure that there will be facilities and space to implement EOR in due course. In many cases, maximum oil recovery is only achieved if EOR is deployed as soon as production begins. A major challenge remains the time delay between the deployment of a given EOR process in a field, often involving considerable extra capital and operational costs, and the response in terms of additional oil production. The benefits from drilling additional water injection wells are usually seen within

months while it may take a year or more before incremental oil resulting from an EOR scheme reaches the production wells.

(3) Further developments are probable in EOR technologies that improve macroscopic sweep. The deep reservoir flow diversion technique described above is designed for water flooding. Similar technologies are required for gas flooding, especially if CO₂ injection for EOR and geological sequestration of the CO₂ is to succeed.

(4) EOR projects are going to become increasingly common worldwide in the future, despite concerns about greenhouse gas emissions, as demand for oil will continue to increase while at the same time it becomes harder to find new oilfields. We have not yet achieved the technological limit in terms of the RF that can be obtained using these processes. At present, their deployment is controlled by economic factors and operational constraints. Research continues to try and mitigate these factors and constraints, as well as to develop more advanced and effective recovery processes, but the challenge in all cases is to move these technologies more rapidly from the laboratory to the field.

References

- Aziz, K. and Gontijo J.E. (1984).: “ A Simple Analytical Model for Simulating Heavyoil Recovery by Cyclic Steam in Pressure-Depleted Reservoirs” , paper SPE 13037.1
- presented at the 59th Annual Technical Conference and Exhibition, Houston.
- Boberg, T.C. and Lantz, R.B. (1966).: “ Calculation of the Production Rate of a Thermally Stimulated Well” , J.Pet.Tech.
- Butler, R.M. and Stephens, D.J., (1980).: “ The Gravity-drainage of Steam-Heated Heavy-Oil to Parallel Horizontal Wells” , paper presented at the 31st Annual Technical Meeting of The Petroleum Society of CIM in Calgary.
- Elliot, K.E. and Kovscek, A.R. (2011): “ Simulation of Early-Time Response of Single-Well Steam Assisted gravity-drainage (SW-SAGD)” , SPE 54618, presented at the Western Regional Meeting of the SPE, Anchorage, Alaska.
- Fontanilla, J.P. and Aziz, K. (2010).: “ Prediction of Bottom-Hole Conditions for Wet Steam Injection Wells” , J.Can.Pet.Tech.

- Jones, J.(2011): “ Cyclic steam Reservoir Model for Viscous Oil, Pressure-depleted, Gravity-drainage Reservoirs” , SPE 6544, 47th annual California Regional Meeting of the SPE of AIME, Bakersfield (April 13-15, 1977).
- Mandl, G. and Volek, C.W.(1996): “ Heat and Mass Transport in Steam-DriveProcesses” , Soc. Pet. Eng. J. pp. 59-79; Trans., AIME, **246**.
- Marx, J.W. and Langenheim, R.H. (1999): “ Reservoir Heating by Hot-FluidInjection” , Trans. AIME 216, 312-315.45.
- Mendonza, H.(2000): “ Horizontal Well Steam Stimulation: A Pilot Test in Western.

APPENDICES

Length [m]	Pressure [Pa]
0	275155.3729
0.380401093	275144.0715
0.760802185	275100.8026
1.52160437	275078.5411
3.046425553	275018.9355
3.300562442	275209.1295
4.571246886	276122.4461
4.761849553	276265.6468
5.333657553	276648.8232
5.52426022	276653.5627
6.858478886	276636.751
8.38330022	276630.1356
8.573902886	276491.2795
9.145710886	276098.8379
9.399847775	275896.3093
10.67053222	274962.8453
11.05173755	274784.6777
12.19535355	274289.5642
12.57551516	274171.9379
13.716	273847.3985

APPENDIX A: Pressure data

Length [m]	Temperature [K]
0	293.2005293
1.52160437	293.201008
3.046425553	293.2026957
4.571246886	293.206978
4.95245222	293.2087203
5.333657553	293.2103822
5.52426022	293.2113385
6.286551165	293.2147976
6.858478886	293.2171772
7.23968422	293.2189093
7.620889553	293.2205458
7.81149222	293.221538
8.573902886	293.2251504
9.145710886	293.2276614
9.399847775	293.2291667
10.67053222	293.236139
11.05173755	293.2387715
12.19535355	293.2462646
12.95567678	293.2478771
13.716	293.2493997

APPENDIX C- Cell

X [m]	Y [m]	Z [m]	Cell volume [m ³]
-1.90554778	-17.25895261	-5.717816673	0.402066121
-1.143137114	-17.25895261	-5.717816673	0.402066121

-0.380726447	-17.25895261	-5.717816673	0.402066121
0.38168422	-17.25895261	-5.717816673	0.402066121
1.144094886	-17.25895261	-5.717816673	0.402066121
1.906505553	-17.25895261	-5.717816673	0.402066121
-1.90554778	-16.567503	-5.717816673	0.401956828
-1.143137114	-16.567503	-5.717816673	0.401956828
-1.90554778	-15.87614738	-5.717816673	0.401956828
-1.143137114	-15.87614738	-5.717816673	0.401956828
-0.380726447	-16.567503	-5.717816673	0.401956828
0.38168422	-16.567503	-5.717816673	0.401956828
-0.380726447	-15.87614738	-5.717816673	0.401956828
0.38168422	-15.87614738	-5.717816673	0.401956828
1.144094886	-16.567503	-5.717816673	0.401956828
1.906505553	-16.567503	-5.717816673	0.401956828
1.144094886	-15.87614738	-5.717816673	0.401956828
1.906505553	-15.87614738	-5.717816673	0.401956828
-1.90554778	-15.18479174	-5.717816673	0.401956858
-1.143137114	-15.18479174	-5.717816673	0.401956858
-1.90554778	-14.49343608	-5.717816673	0.401956858
-1.143137114	-14.49343608	-5.717816673	0.401956858
-0.380726447	-15.18479174	-5.717816673	0.401956858
0.38168422	-15.18479174	-5.717816673	0.401956858
-0.380726447	-14.49343608	-5.717816673	0.401956858
0.38168422	-14.49343608	-5.717816673	0.401956858
1.144094886	-15.18479174	-5.717816673	0.401956858
1.906505553	-15.18479174	-5.717816673	0.401956858
1.144094886	-14.49343608	-5.717816673	0.401956858
1.906505553	-14.49343608	-5.717816673	0.401956858
-1.90554778	-17.25895261	-4.95531825	0.401973542
-1.143137114	-17.25895261	-4.95531825	0.401973542
-1.90554778	-17.25895261	-4.192907624	0.401973542
-1.143137114	-17.25895261	-4.192907624	0.401973542
-0.380726447	-17.25895261	-4.95531825	0.401973542
0.38168422	-17.25895261	-4.95531825	0.401973542
-0.380726447	-17.25895261	-4.192907624	0.401973542
0.38168422	-17.25895261	-4.192907624	0.401973542
1.144094886	-17.25895261	-4.95531825	0.401973542
1.906505553	-17.25895261	-4.95531825	0.401973542
1.144094886	-17.25895261	-4.192907624	0.401973542
1.906505553	-17.25895261	-4.192907624	0.401973542
-4.573985038	-16.22182519	-4.574112937	3.214913878
-3.04916378	-16.22182519	-4.574112937	3.214914195
-1.90554778	-16.567503	-4.95531825	0.401864274
-1.143137114	-16.567503	-4.95531825	0.401864274
-1.90554778	-15.87614738	-4.95531825	0.401864274
-1.143137114	-15.87614738	-4.95531825	0.401864274
-1.90554778	-16.567503	-4.192907624	0.401864274